Confinement of the antitumoral drug cisplatin inside edge-functionalized carbon nanotubes and its release near lipid membrane

Alia Mejri, Bahoueddine Tangour, Guillaume Herlem, Fabien Picaud

Confinement of the antitumoral drug cisplatin inside edge functionalized carbon nanotubes and its release near lipid membrane

Alia MEJRI[1,2], Bahoueddine TANGOUR[1], Guillaume HERLEM[2] and Fabien PICAUD[2]*

[1] Université de Tunis El Manar, Unité de Recherche de Modélisation en Sciences Fondamentales et didactiques, Equipe de Chimie Théorique, BP254, El Manar 2, 2096, Tunisia.
[2] Laboratoire de Nanomédecine, Imagerie et Thérapeutiques, EA4662, UFR Sciences et Techniques, Centre Hospitalier Universitaire et Université de Bourgogne Franche Comté, 16 route de Gray, 25030 Besançon.

Abstract

Platinum complexes are active anti-tumor agents. They are widely used in chemotherapy medication for the treatment of several cancer types. Unfortunately, these drugs present poor stability when administered and have several side effects, damaging healthy cells around the tumor. One way to remedy the damage is to confine drug molecules in carbon cages such as carbon nanotubes (CNTs) before delivering them near their target cells. In order to open their ends, the CNTs must be functionnalized by oxidation. This leads to the saturation of the carbon dangling bonds with an alcohol functional group, for instance.

In this study, molecular dynamics simulations are carried out to assess the influence of CNT's chemical functional groups (-H, -OH, -COOH) on the retention time and release processes of cisplatin molecules throughout the process of vectorization to a cell membrane.

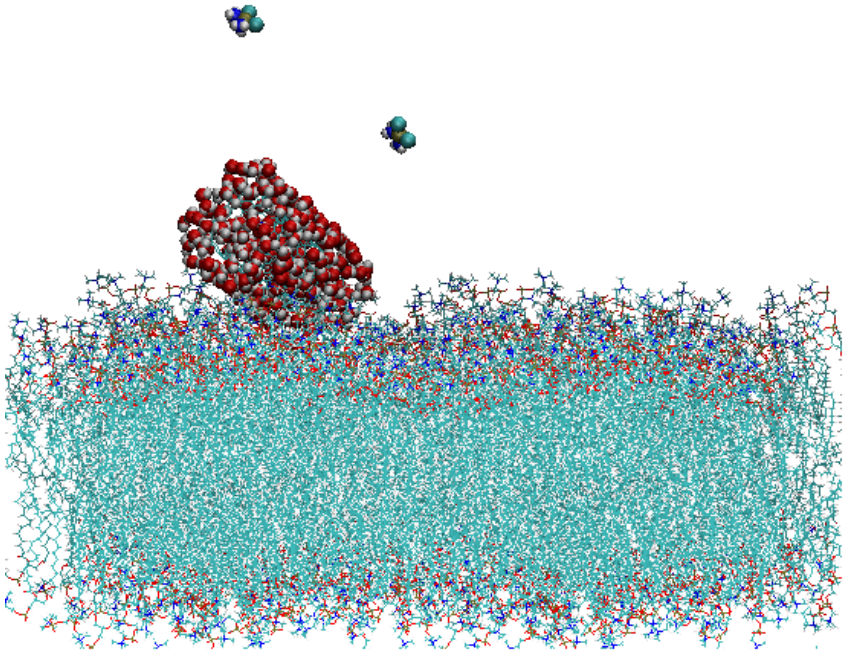

Keywords: CNT, POPC membrane, encapsulation, functionalization, platinum complex.

1. Introduction

Carbon nanotubes (CNTs) have opened up many amazing opportunities in the field of medicinal research. These hollow structures with a large internal surface allow can accommodate small molecules [1-3] arousing the interest of researchers on the confinement and storage of many chemical elements such as water [4-6] H_2, or F_2 for various applications [7-14]. These structures are also very promising drug vectors for purely therapeutic purposes [15-20]. CNTs are used as drug carriers during their transfer to the target cells. This strategy aims to significantly reduce the side effects of the treatment and to prevent the drugs from degradation before they reach the organs [21-23]. Cisplatin (CDDP) is a well-known platinum complex widely used in the treatment of various types of cancers [24, 25]. However, it is very unstable when administered causing damage to safe cells, particularly those close to those targeted [26, 27] and leading to many side effects.

To overcome the CDDP cytotoxicity , the solution proposed by many scientists is to confine it in the different structures such as polymers, liposomes, micelles or dendrimers [28-32], and various types of solid capsules such as boron nitride (BNNTs) [33-40] or carbon nanotubes [41-45].

Frequently during their synthesis, CNTs are closed and quite difficult to disperse in an aqueous solvent making their filling impossible [46, 47]. To overcome this situation, it is necessary to perform an oxidation step to open, cut and functionalize these structures as required. This process can be done either by thermal oxidation of CNTs, by heating in the presence of oxygen in the air and at temperatures ranging from 350 to 500°C[48] or by chemical oxidation using oxidizing agents. Oxidative cleavage gives oxygen function at the ends of CNTs, such as alcohol or carboxylic acid functions [49-51].The latter make it possible to improve both the miscibility and the dispersion of the CNT in various media with very precise pH conditions.

The purpose of this molecular dynamics (MD) study is to assess the influence of edge chemical functional groups on the entry/exit capacity and retention time of cisplatin molecules within the carbon structure. In this study, we used a zigzag type SWCNT, denoted as (17,0) since its diameter is optimal

to contain the maximum number of drug molecules (for a tube length equal to 20 Å) [41]. The insertion process consisted of a gradual introduction of cisplatin molecules (1 to 4) inside an unfunctionalized carbon nanotube [41]. Here, we will focus on the effect of chemical functional groups added to dangling carbon atoms on the residence times of CDDP molecules inside the carbon cage. This will be analyzed in terms of time of entry and exit of these molecules and of solvation inside the cargo. The main interactions felt by CDDPs during the different processes will be also investigated. Our reference system is (17,0) CNT, filled with CDDP molecules, the ends of the tubes are saturated with hydrogen atoms. Then, we will gradually increase the size of the chemical functional groups, changing –H to –OH and then to –COOH groups, respectively. The release of drug molecules near POPC lipid bilayer will be finally studied to understand the different energy contributions that govern this phenomenon.

2. Calculations details and system model

Cisplatin molecule geometry has been optimized using the density functional theory as part of the Gaussian 09 package[52]. B3LYP functional [53-56] with a 6-31g (d, p) basis set [57] was used for all atoms except for platinum atom which was represented by the LanL2DZ basis set [58]. The RESP charges and the Hessian matrix were also extracted to perform molecular dynamics simulations. The methodology for constructing force field parameters for CDDP molecules is based on a combination of quantum mechanics and molecular mechanics methods leading to a complete description of the platinum complex. The procedure was detailed by Norrby et al. [59]. The MD simulations were conducted in a statistical mechanical ensemble NPT where the temperature was kept at 300 K using Langevin dynamics and the pressure was set at 1atm using the Langevin pistonPeriodic boundary conditions were used for all the simulations in order to get rid of any boundary effects. The calculations were performed using the NAMD code[59]. In this framework, the integration time was equal to 1 femtosecond to correctly describe the water dynamics that occurs at a subpicosecond scale

[60]. The particle mesh Ewald (PME) summation was used to calculate periodic electrostatic interactions of the complete system.

The different systems studied were immersed in a cubic TIP3P [61] water box with 0.15M NaCl salt. The TIP3P water model exhibits partial atomic charges centered on hydrogen and oxygen atoms. It has a rigid geometry which is consistent with water in the liquid phase. Moreover, TIP3P well predicts the density and enthalpy of vaporization of water under ambient conditions. On the other hand, Charmm36 force field has been well validated for the TIP3P water model, in particular to correctly reproduce the properties of the lipid bilayer which are very sensitive to the water model [62].

A zigzag single-walled CNT (17,0) was selected with a diameter of 0.13 nm and the tube length was set at 20 Å. The simulated water box dimensions for the CNT-H, CNT-OH and CNT-COOH systems are respectively (54,55,71) A^3, (55,55,75) A^3 and (56,56,78) A^3. The Lennard Jones potential parameters describing C-C, C-O and C-H forces were also taken into account in the simulation parameters. They were chosen as coming from the Charmm36 force field. All these parameters are detailed in the supplementary materials section (S1) and (S2). Note here that the dynamics of the CNT should be taken into account using current existing model (such as the Brenner-Tersoff potential) [63]. This last model can model the mechanical deformations of the CNT body according to the environment appearing in the simulation or model the CNT growth. Here, we are not interested in the elasticity or in the viscosity of the CNT. In our previous work, the CNT was described as a fixed structure [36]. Here CNT can move through the volume of the box as a quasi-rigid entity since bond and angle parameters remain very large.

To estimate the free energy barrier that the CDDP must cross to exit from the inner volume of the CNT, we used the adaptive biasing force (ABF) method [64, 65] in NAMD formulation and implementation [66]. This method was developed by Darve et al. [67] and has been largely used in the exploration of reaction path coordinates and free energy calculations [68]. This method is based on the application of an external biasing force at each step of the simulation allowing the molecule to

overcome significant energy barriers and escape the minima of the free energy landscape along the reaction coordinate ξ [69]. The reaction coordinate is representative of the observable phenomenon: in our study it is the distance traveled by the molecule (initially placed near the tube) to cross the entire carbon cage and exit. The total distance of 32 Å was sampled in 8 consecutive 4 Å windows with bins of 0.1 Å.

The energy profiles in fig. 6 were obtained from ABF equilibrium simulations totaling 18 ns of sampling for each window, via an integration of the force applied to the cisplatin along the tube axis.

The lipid bilayer was simulated under the same solvent conditions. It consisted of 176 1-palmitoyl-2-oleoyl-sn-glycero-3-phosphocholine (POPC) lipids, used to mimic the inner lipid leaflet of membranes. POPC is often modeled in Molecular Dynamics calculations to simulate the biological environment particularly in the context of an interaction with a drug molecule. There is many theoretical works in this field [18, 40, 70, 71]. The POPC force field is taken from the Charmm36 lipids database.

Moreover, the membrane is relaxed beforehand for 40 ns in a water box size of (250,206,203) $Å^3$. The system contained around 6000 water molecules. This preliminary simulation aims to stabilize the hydrophilic parts of the lipid bilayer because it is a complex assembly from a composition point of view. It presents heterogeneous regions with varying thicknesses and channel lengths. Suitable relaxation time would avoid structural tensions due to cohesions between amino acid channels.

3. Results and discussion

The work presented in this paper is divided into two complementary parts. The first deals with the effects of the CNT functionalized edge on the entry or exit of CDDP molecules. The second focuses on the interaction between a released molecule and the membrane.

3.1. Edge saturation

Saturation by hydrogen atoms

Four CDDP molecules were encapsulated in the CNT prior to system solvation. Then, minimization and thermalization were conducted for 5ns before launching the production runs. During these, many energy contributions are felt by the CDDP drug molecules, they have been divided into three terms: the lateral molecule-molecule (CDDP-CDDP), the solvation (CDDP-water), and the confinement (CDDP-CNT) pair interactions. All these interactions have been described by pair energies (such as van der Waals and electrostatic terms) averaged by the total number of frames kept for production runs.

Fig. 1 shows these different terms for CDDP molecules during the simulation. The lateral energy between CDDP molecules varies between -14.0 and 0.0 kcal/mol. The four molecules adopt certain positions which can result in a more stable cluster formation than isolated molecules. This cluster formation is observed in other similar studies (Tripisciano et al.) where CDDP clusters formed inside the internal hollow area of MWCNTs [72]. These clusters were also characterized using electron-dispersion spectroscopy (EDS) inside an ultrashort single-walled carbon nanotube by Guven et al. [73] DeSouza et al. also experimentally observed the cluster form of CDDP drugs confined within a SWCNT of radius 10-20 Å [74]. In addition, the tube wall exerts a strong stabilizing interaction for CDDP with value ranging from -35.0 to -15.0 kcal/mol, depending on the confined molecule number.

However, according to fig. 1, the most stabilizing interaction for the confined cisplatin molecule throughout the simulation is due to the solvation of the molecule. The corresponding energy fluctuates around -144 kcal/mol up to 8 nanoseconds before decreasing to -240kcal/mol when the first molecule leaves the CNT. We can therefore relate the stability of the drug molecules inside the cage to their solvation by water. Limiting it would probably decrease their residence time.

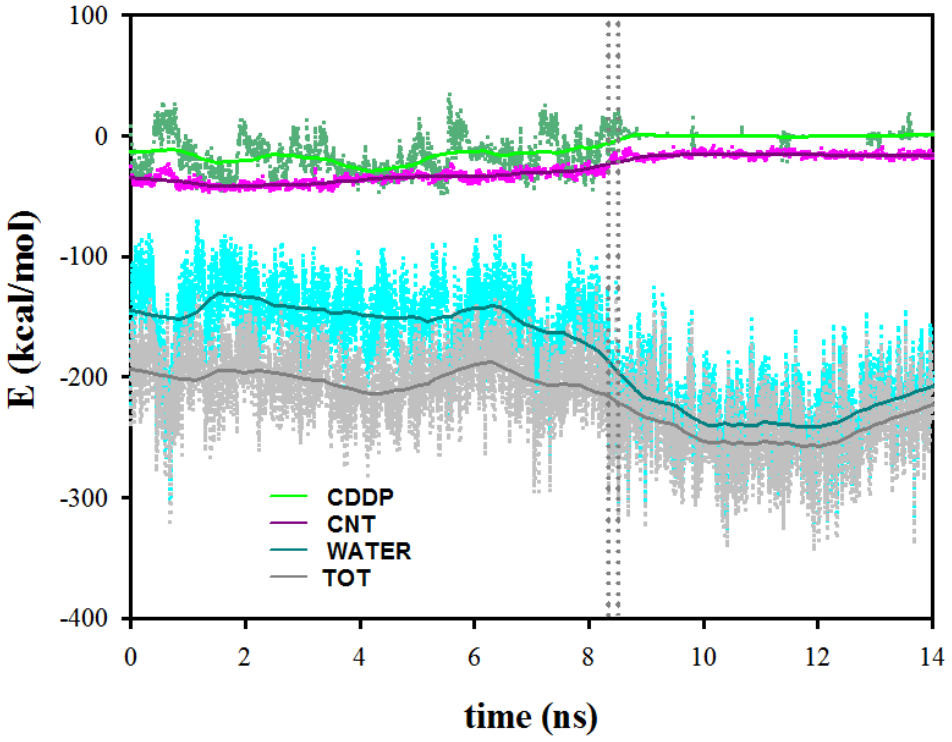

Fig. 1. Energy contributions felt by CDDP in the hydrogenated end (17,0) tube. a) CDDP-CDDP, b) CNT-CDDP, c) CDDP-water and d) Total energy. Dotted lines represent the exit times of the 1st and 2nd CDDP molecules, respectively.

The tracking of the movement of the CDDP molecules indicates that the 4 CDDP molecules remain confined for 8.32 ns. Beyond this time, a first molecule leaves the cage followed by the second one at 8.38 ns as shown in fig. 2.

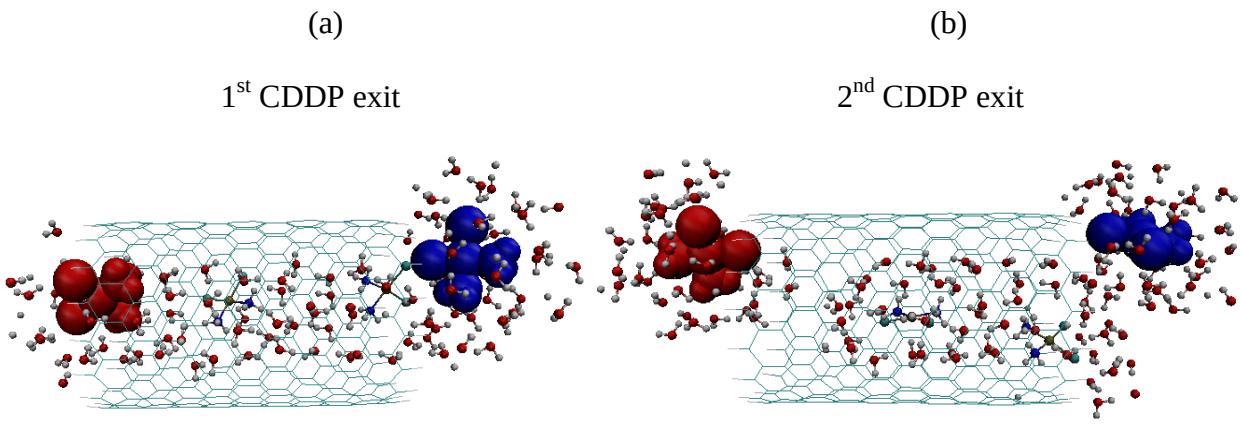

Fig. 2. Exit phenomena of the two CDDP molecules from the saturated carbon nanotube.

The interaction between CDDP molecules and water remains stable and fluctuates slightly around -144.0 kcal/mol. These two close outputs significantly influence the energy curve of the water interaction with cisplatin by a stronger stabilization of this interaction at -240.0 kcal/mol. This is due to the high solvation of CDDP molecules inside and outside the cage.

Fig. 3 shows the number of water molecules when four molecules are confined in CNT and when two of them leave the cargo ship. This number increases from 7 to 8 molecules, reflecting an improvement of the molecule solvation in the cage.

Furthermore, the CDDPs were arranged in a plane parallel to the inner wall of the tube, which generates a large space filled with water. This strongly stabilizes the drug molecules. At the same time, CDDPs try to stabilize by returning to the center of the tube, in a clustered preferential position grouped in the center of the tube (Fig 3c-d). In our previous study, the same number of cisplatin molecules were introduced inside a tube with unsaturated and non-functionalized terminations of identical diameter and length. The CDDP-water interaction fluctuated around -200 kcal/ mol [41], which was slightly lower than here.

The CDDP molecules do not pass outside the tube in the first part of simulation (from 0 to 8.32 ns). Indeed, the lateral and confinement interaction stabilize them. From Fig. 3c we can observe that the NH_2 functional groups of CDDP molecules are inside the tube. Indeed, we believe that a cluster of drug molecules can be created, helping to stabilize each other inside the cage [72, 75, 76]. The exit phenomena can occur when the water molecules enter the tube. As the number of water molecules increases inside the cage due to the CDDP organization, the CDDP molecules move away from each other and jostle, promoting a first exit to re-stabilize. The establishment of hydrogen bonds therefore play a key role in this situation. As soon as these hydrogen bonds will be broken by the water entering the tube, the drug release will be progressively observed.

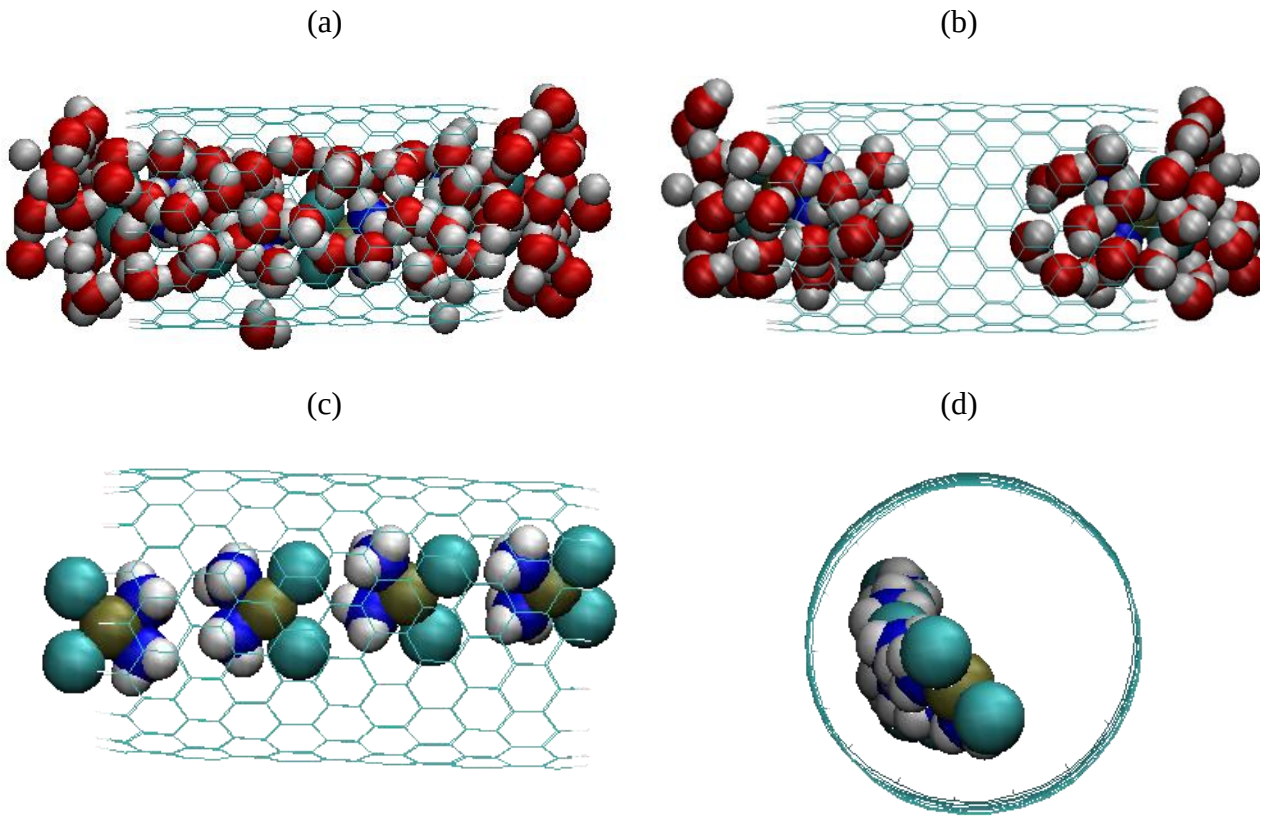

Fig. 3. a) 7 water molecules around each CDDP b) 8 to 9 water molecules around each CDDP c) and d) cluster conformation of drug molecules.

It was also interesting to look at the arrangement of water molecules around the different CDDP molecules during their confinement. For this we have extracted from the production runs of the MD simulations, the radial distribution functions g (r) and its integral number N(r) for the first and the second solvation peaks of Table 1. The g(r) functions were calculated as the average of particles pairs distances between CDDP and water molecules. N(r) is the integral number $\int_0^r \rho\, g(r) r^2$ dr for all pairs of atoms with a resolution of 0.1 Å and a maximum r of 10 Å. As can be viewed in Table 1, the modification of the edge function of the carbon nanotube by –H atoms, did not radically change the different physical observables that we determined in this study.

Table 1 also summarizes the different retention times noted for the three systems investigated in the this study. The retention time given here is defined as the time for which the four cisplatin molecules are confined together inside the carbon cage.

Table 1: Integral number for the first and second peaks of the radial density functions between CDDP and water inside the nanotube (as shown in Fig. 11).

Tube termination	**-C-**	**-H**	**-OH**
N(first g(r) peak)	5.8	7.7	5
Retention time (ns)	7.50	8.32	>14.00

3.1.1. CNT edges functionalized by -OH and -COOH groups

When the tube ends are oxidized by –COOH groups, only three molecules of CDDP can enter the tube. The fourth could not access it. We suspect, on one hand, that this molecule is repelled by -COOH groups, which prevent it from accessing the tube, and on the other hand, that the solvent effect is very pronounced in this situation, favoring a difficult drug entrance in the cage. Whatever the reason, this functionalized CNT does not seem to be the most suitable for vectorizing the anticancer drug since certain molecules will have to be left free outside the nanovector.

In the case of tube edges oxidized by -OH, fig. 4 shows the different energies felt by the CDDP molecules during a simulation lasting 14 ns. All these energy variations show an overall stabilization of the system during the simulation. This is because the CDDP drug molecules themselves aggregated (see Fig. 5 showing a simulation snapshot during the simulation (at t= 7.7 ns)) and lower their respective energies, as shown in Fig. 4. The energy felt by CDDPs oscillates between -46.0 and -21.0 kcal/mol. The graph also reveals that the affinity of CDDP with the inner wall of CNT remains constant throughout the simulation and equal to about -80.0 kcal/mol.

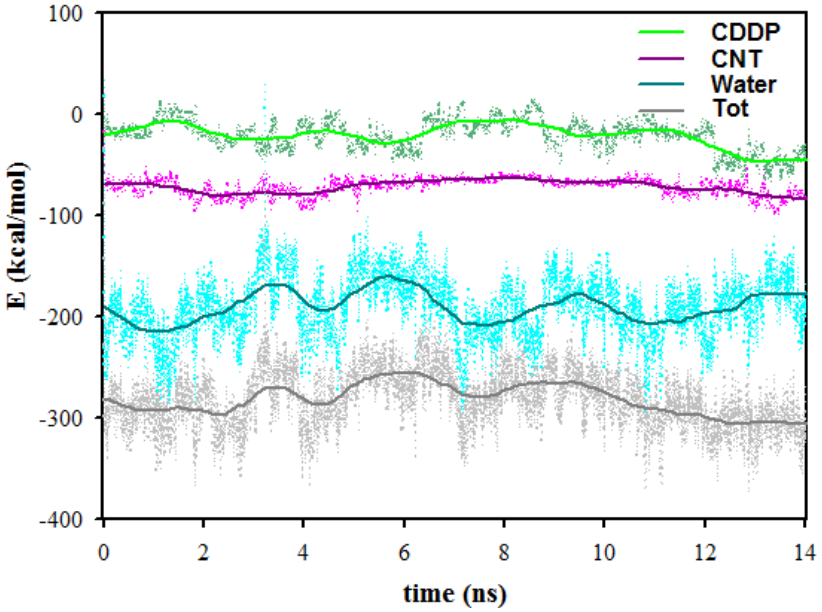

Fig. 4. Total energy contributions felt by cisplatin in the hydroxyl-terminated tube (17,0). In green is shown the lateral interaction between CDDP molecules, in pink is plotted the confinement interaction between CDDP molecules and CNT, in blue the solvation interactions between CDDP and water. The total energy of the system is shown in gray.

The greatest contribution comes, as before, from the solvent (water), with an average value of the pair energy which does not vary too much during the simulation and remains around -200.0 kcal/mol.

In order to better study the role of water molecules, as well as their behavior during simulation, we calculated the water radial density around the CDDP molecules. The g(r) and N(r) plots reveal that an average of 7.4 water molecules surrounds each CDDP drug molecule inside the CNT during the simulation.

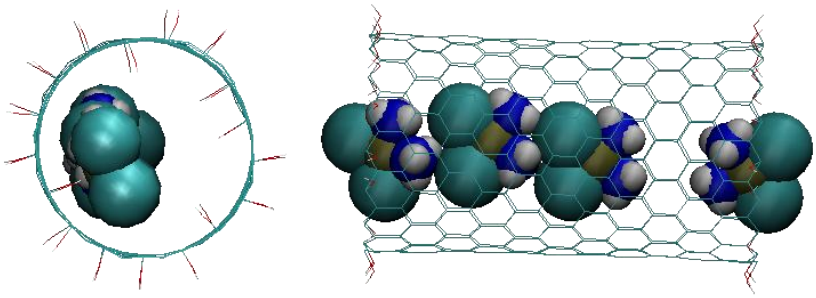

Fig. 5. Four cisplatin molecules interacting with the inner wall of the tube.

During this simulation time, none of the four molecules of cisplatin leaves the carbon cage and we can consider that the retention time is in this case greater than 14.00 ns. To confirm this, we have performed ABF simulations of a CDDP molecule to leave the CNT, depending on its edge functionalization. Fig. 6 presents the different FEP obtained along the carbon nanotube axis for the three simulated configurations (dangling bonds, bonds functionalized with –H atoms, or –OH atoms).

Due to the symmetry of the molecule, the graph shows two separate energy barriers for the cisplatin entry for each case. The smaller ones are equal to about 1.1 kcal/mol for the unsaturated carbon nanotube, 2.3 and 3.3 kcal/mol for the CNT-H and CNT-OH tubes, respectively. These amounts represent the smallest energies that a drug molecule must provide, at least, to get out of the carbon cage. Note that this result is comparable to an earlier study undertaken by Wolski et al. wherein doxorubicin is highly conserved in a tip-functionalized carbon nanotube with polyethylene glycol and folic acid. Indeed, the exit free energy barrier is practically multiplied by 10 when the ends of the tube are functionalized [77, 78].

These results deal with the residence times obtained previously, in particular for the tube with the -OH terminations for which there are no phenomena of cisplatin exits during the entire simulation.

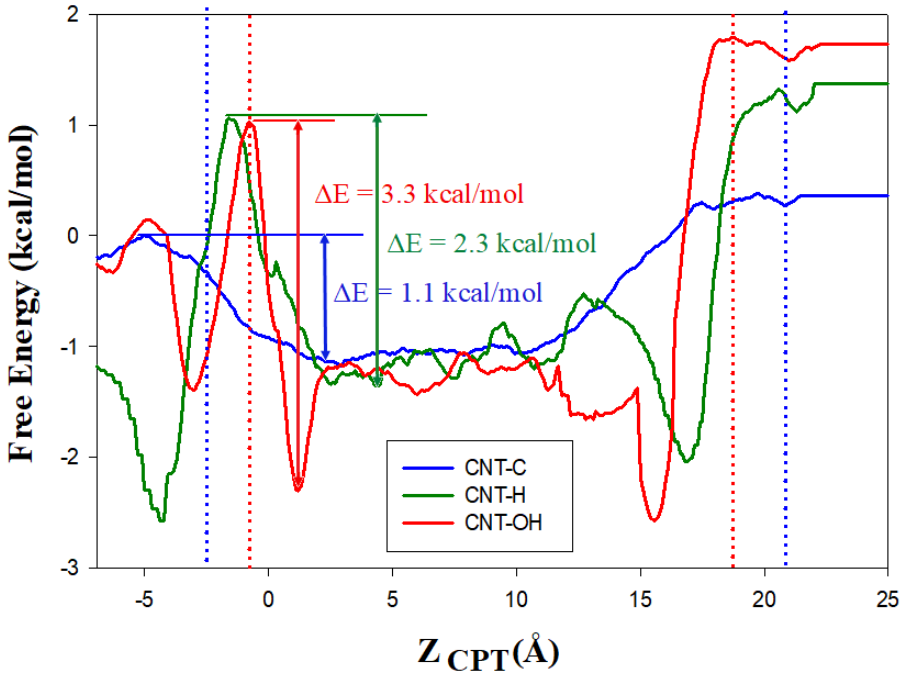

Fig. 6. Free energy profiles for cisplatin molecule transporting through the danglind bonds CNT-C (blue solid line), CNT-H (green solid line) and CNT-OH (red solid line) with respect to tube axis Z_{CPT}. Dotted lines in red delimits the tube extremities (carbon atoms); dotted lines (in blue) indicates the saturating –OH bonds positions. This profile was obtained from equilibrium ABF simulations and integration of the force applied on cisplatin along the z-direction of the Cartesian space.

On the other hand, we calculated the probability that the drug leaves its carbonaceous cage in the three situations. Based on the transition state theory [79], we can determine the hopping rate of the molecule out of the nanotube as proportional to the exponential of the free energy barrier on thermal energy at 300K. Assuming the same prefactor, the ratio of the departure probability for that drug molecule becomes a simple Arrhenius law that depends on the barrier energy difference for each situation. As a consequence, a 40 times greater hopping rate is obtained for dangling bonds of the carbon nanotube compared to the hydroxylated tube. Likewise, the hopping rate of the drug leaving the tube at the hydrogen saturated ends is 5.3

that of its hydroxylated counterpart. This also corroborates the observation made in the simulations.

The long residence time of the CDDP molecules inside the tube ended with -OH functional groups, makes this system the most appropriate for studying it under biological conditions. This system has thus been approached from a biological membrane in order to evaluate the time of release of molecules near the membrane.

1.1. CDDP-CNT-OH system interaction with POPC-type biological membrane

The system consisting of four CDDP molecules confined in the –OH functionalized CNT was placed at a distance of 25 Å from the biological membrane. The membrane was previously relaxed for 40 ns to optimize its lateral dimensions and to avoid the apparition of unexpected dynamic effects. The entire system was then solvated in a water box of (250,206,203) $Å^3$ for a 144 ns MD simulation. Fig. 7 indicates the most important pair interaction energies felt by the drug molecules during the simulation.

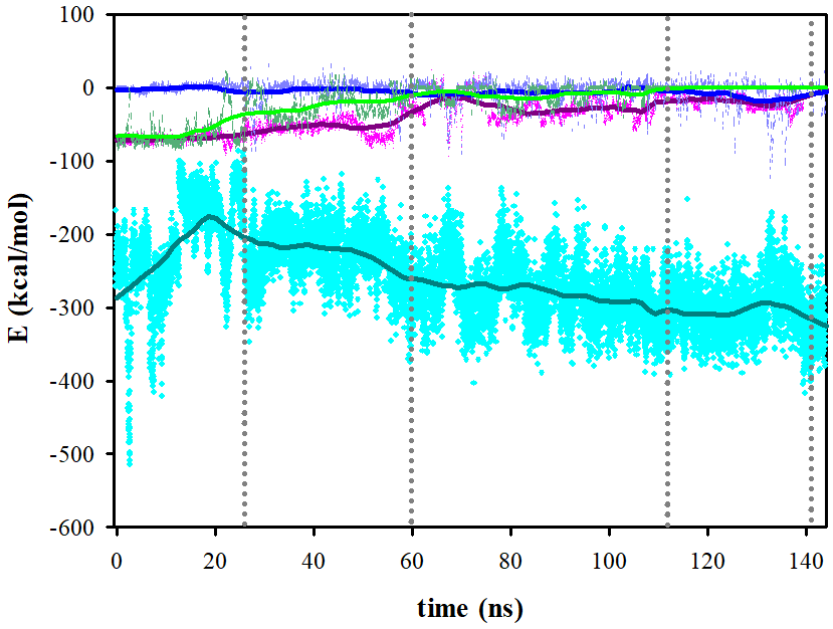

Fig. 7. Total energies contributions felt by cisplatin during simulation. Dotted lines indicates the exit of CDDP molecules from the cage. In green lateral CDDP-CDDP interaction, in pink confinement CDDP-CNT interaction, in blue solvation CDDP-water interaction.

The simulation was launched until the exit of all the confined molecules from the tube was effective. The different phases of the simulation can be separated as follows. First, all CDDP are held inside the CNT until the drug nanovector reaches the POPC membrane. From this situation, the CNT lied to the membrane and strongly interacted with it. For a perfect CNT alone, the next step is to try to insert inside the membrane. However, the presence of both –OH groups and the CDDP molecules appears to delay this phenomenon. Therefore, we never observed CNT insertion throughout the simulation. Instead of that, the CDDP molecules were progressively released from the CNT into the water where they can diffuse near the membrane. However, as shown in fig. 7, the interaction of CDDP molecules with the POPC membrane has never been too important.

To analyze the approach of the CNT to the membrane during the simulation, we plot in fig. 8 the interaction energy between the CNT and the POPC. It can be observed that the CNT adopts different positions ranging from parallel and perpendicular orientation compared to the membrane. These fluctuations come from the attraction of the CNT with the POPC. Indeed, we have observed that each CDDP release step is preceded by a vertical conformation of the tube to prepare the release of the drug molecule (as depicted in fig. 9). Note that the CDDP-POPC interaction stabilized at -6.5 kcal/mol at the end of the simulation indicating the release of all the drug molecules close to the membrane cell.

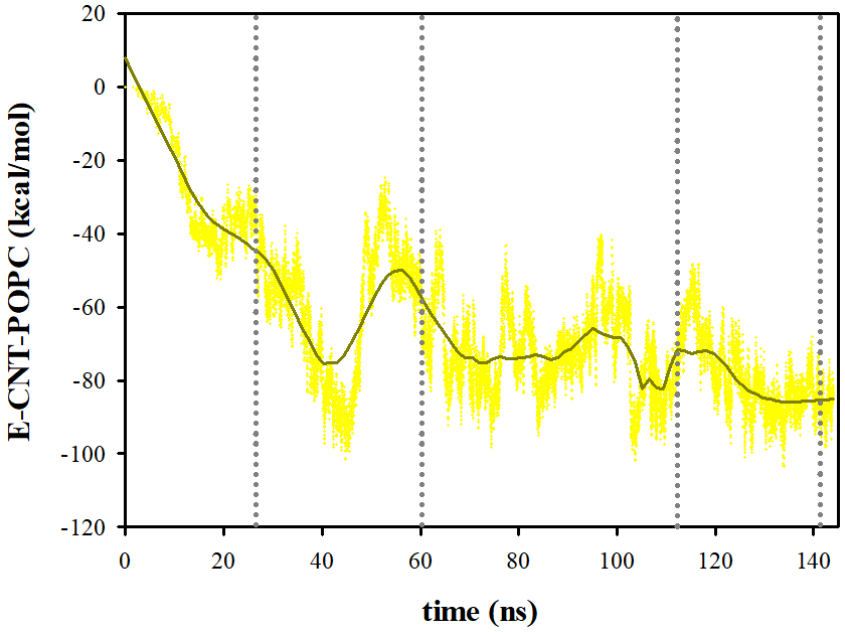

Fig. 8. Variation of CNT-POPC membrane interaction. Dotted lines indicate the exit of CDDP.

(a) (b)

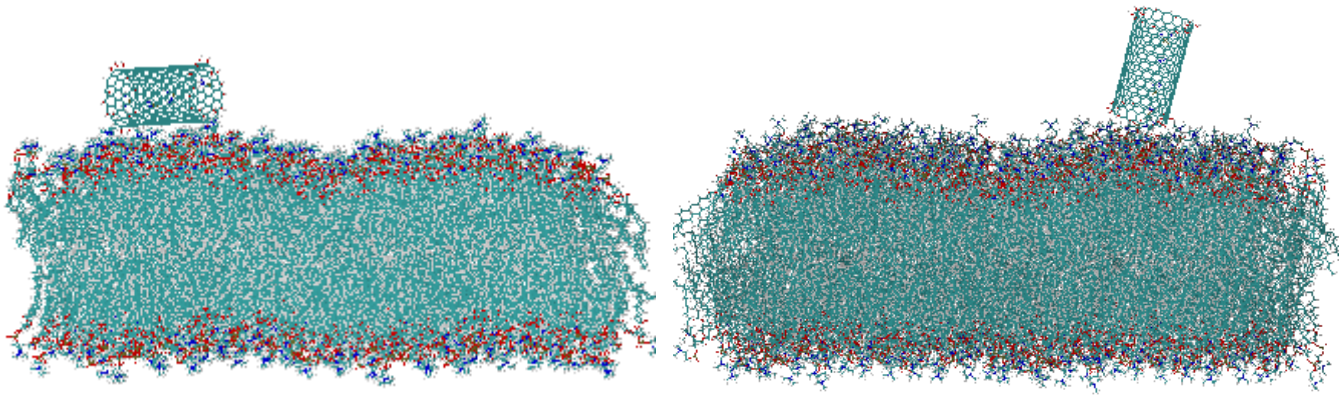

Fig. 9. CNT conformations near membrane cell.

All the steps are depicted in fig. 10. In fact, the drug exit times are about 26., 60., 112. and 141. ns, respectively. The retention times of the drug molecules are thus much greater than those observed previously [41].

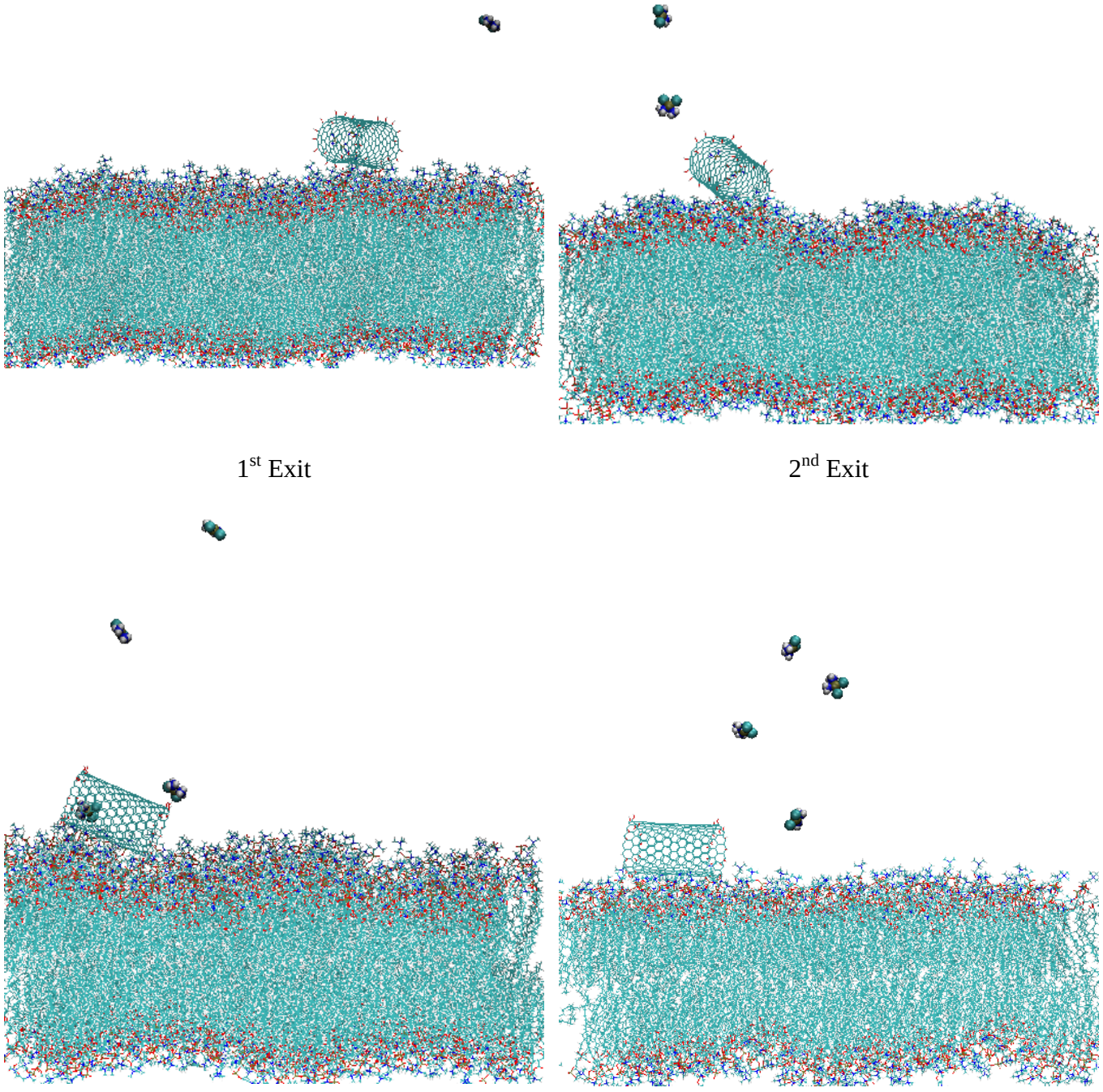

Fig. 10. Exit steps of CDDP molecules during the simulation

The increase in molecular residence time comes from the functionalization of the CNT edge that maintained the molecule inside the CNT. But we can also notice in fig. 7 that the solvation (CDDP-water) interaction remains the most stable, as observed without the

membrane cell. It varies between -285.0 and -324.0 kcal/mol depending on the simulation time. This interaction gradually decreased as the number of molecules inside the CNT also decreased. Indeed, the departure of each drug molecule was accompanied by a significant solvation of its other counterparts inside the tube due to the insertion of supplementary water molecules into the internal space of the cage. The gradual rearrangement of the water molecules inside the tube makes the study very interesting because it allows a "step by step" delivery of the drug molecules near to the targeted cell resulting in the design of an efficient therapeutic tool for drug delivery

The radial density distribution calculation (fig. 11) is plotted to estimate the number of water molecules around drug molecules inside and outside the tube. When CDDPs are kept inside the tube, a water shell around 5 Å is observed. This peak corresponds to 7.4 water molecules. In the opposite case (CDDP outside the CNT), the first water shell runs up to 4.58 Å, corresponding to a total number of water molecules equal to 8.74.

(a)

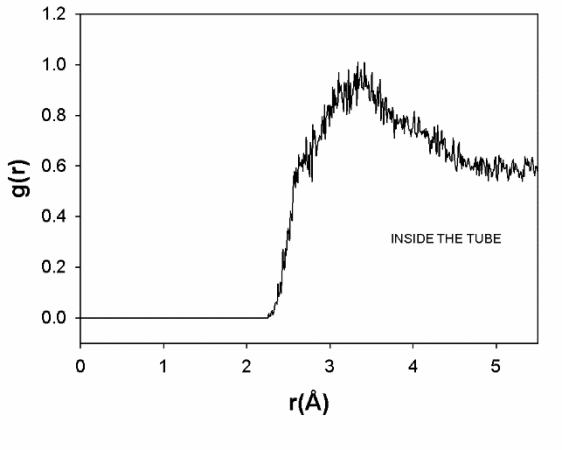

(b)

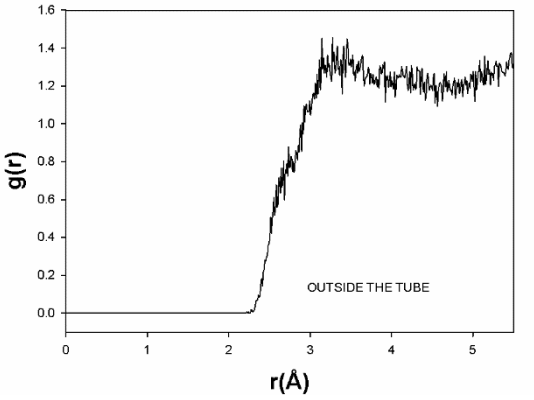

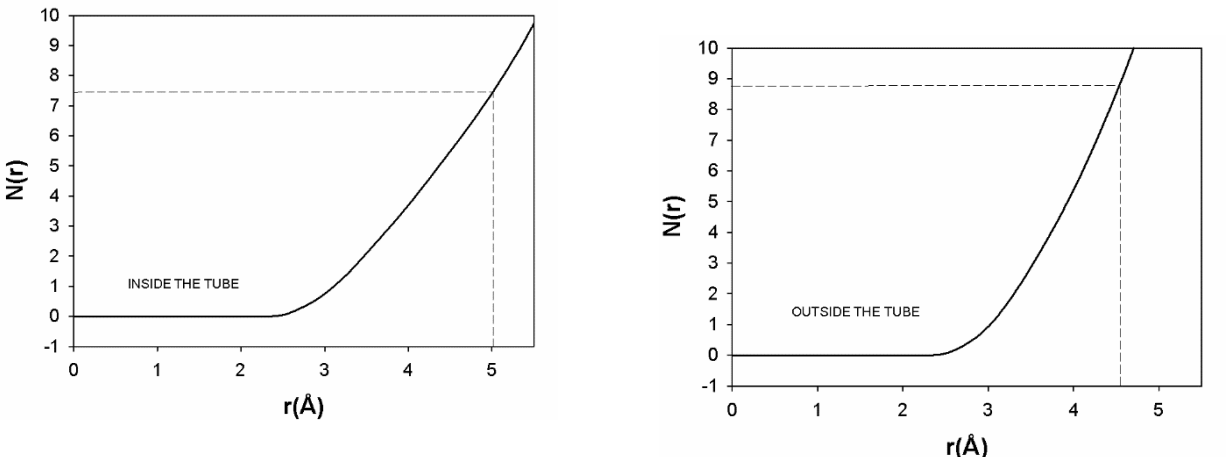

Fig. 11. Radial density function between CDDP and water molecules and their integration (a) inside and (b) outside the tube.

The arrangement of the water molecules around CDDP is depicted in fig. 12. The water molecules are arranged in a pseudo-sphere around the drug molecules. The number of water molecules constituting these spheres varies from 7 to 9 water molecules when the CDDP molecules are drawn from the carbon cage. The improvement in the solvation of the drug outside the cage and the significant water-CDDP interaction pushes other drug molecules to leave the carbon cage at higher simulation times.

(a) (b)

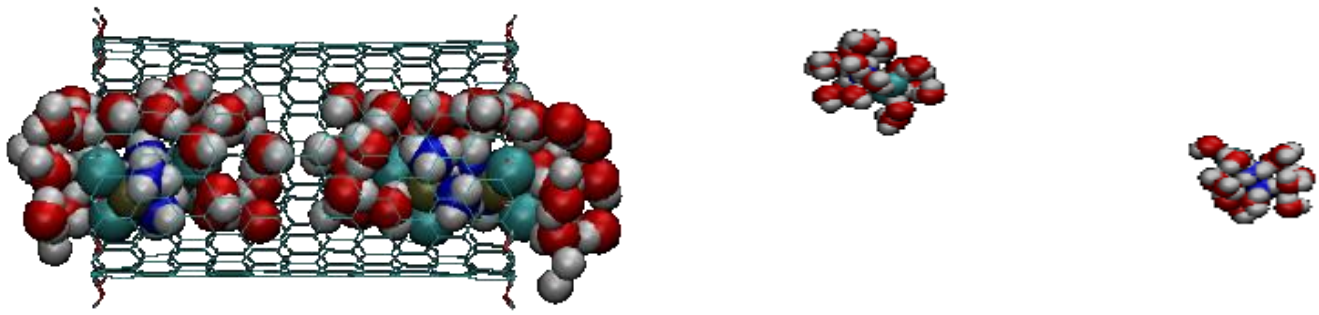

Fig. 12. Arrangement of the water molecules around CDDP (a) inside and (b) outside the tube

2. Conclusion

We propose in these MD simulations to investigate the behavior of an optimal CNT nanovector filled with anticancer drug molecules. Using different functionalizations of the CNT edges, we have shown that the most suitable cargo for these molecules is obtained by functionalization of CNT dangling bonds with –OH groups . In fact, this system allows an easy access to CDDP molecules and significantly increases their retention times. Moreover, no release phenomenon was observed during transport of the cargo to the cell membrane. This is because the gradual release of the active drug molecules is only possible when the CNT tries to enter the lipid membrane. This work opens a very interesting way in using the CNT as a good potential drug nanovector for stable therapeutic nanovectorization and transport.

Acknowledgement

Calculations were performed with the supercomputer regional facility Mesocenter of the University of Franche-Comté.

Author contribution statement

All the authors were involved in the preparation of the manuscript. All the authors have read and approved the final manuscript.

References

1. D. Tasis, N. Tagmatarchis, A. Bianco and M. Prato, *Chemical Reviews*, **106**, 1105, (2006).
2. S. Manzetti, *Advances in Manufacturing*, **1**, 198, (2013).
3. A. Peigney, C. Laurent, E. Flahaut, R. Bacsa and A. Rousset, *Carbon*, **39**, 507, (2001).
4. V. V. Chaban and O. V. Prezhdo, *ACS Nano*, **5**, 5647, (2011).
5. X. Pan and X. Bao, *Accounts of Chemical Research*, **44**, 553, (2011).
6. N. Naguib, H. Ye, Y. Gogotsi, A. G. Yazicioglu, C. M. Megaridis and M. Yoshimura, *Nano Letters*, **4**, 2237, (2004).
7. W. F. Gtari and B. Tangour, *International Journal of Quantum Chemistry*, **113**, 2397, (2013).
8. S. Lee, K.-S. Park, Y. C. Choi, Y. Park, J. M. Bok, D. J. Bae, K.-S. Nahm, Y. G. Choi, S. C. Yu, N. Kim, T. Frauenheim and Y. H. Lee, *Synthetic Metals*, **113**, (2000).
9. H. Dodziuk and G. Dolgonos, *Chemical Physics Letters*, **356**, 79, (2002).
10. T. Takenobu, T. Takano, M. Shiraishi, Y. Murakami, M. Ata, H. Kataura, Y. Achiba and Y. Iwasa, *Nature materials*, **2**, 683, (2003).
11. L. Schlapbach and A. Züttel, *Nature*, **414**, 353, (2001).
12. H.-M. Cheng, C. Yuan and C. Liu, *Carbon*, **39**, 1447, (2001).
13. A. C. Dillon, K. M. Jones, T. A. Bekkedahl, C. H. Kiang, D. S. Bethune and M. J. Heben, *Nature*, **386**, 377, (1997).
14. W. F. Gtari and B. Tangour, *Canadian Journal of Chemistry*, **94**, 15, (2016).
15. M. Martincic and G. Tobias, *Expert opinion on drug delivery*, **12**, 563, (2015).
16. Z. Khatti, S. M. Hashemianzadeh and S. A. Shafiei, *Adv Pharm Bull*, **8**, 163, (2018).
17. L. Zhang, G. Peng, J. Li, L. Liang, Z. Kong, H. Wang, L. Jia, X. Wang, W. Zhang and J.-W. Shen, *Journal of Molecular Liquids*, **262**, 295, (2018).
18. M. Pakdel, H. Raissi and M. Shahabi, *Journal of Biomolecular Structure and Dynamics*, **38**, 1488, (2020).
19. M. Yoosefian, S. Sabaei and N. Etminan, *Computers in Biology and Medicine*, **114**, 103433, (2019).
20. J. Chen, D. Mao, X. Wang, G. Zhou, S. Zeng, L. Chen, C. Dai and S. Feng, *The Journal of Physical Chemistry C*, **123**, 9567, (2019).
21. K. Ajima, T. Murakami, Y. Mizoguchi, K. Tsuchida, T. Ichihashi, S. Iijima and M. Yudasaka, *ACS Nano*, **2**, 2057, (2008).
22. A. Rajeswaran, A. Trojan, B. Burnand and M. Giannelli, *Lung cancer (Amsterdam, Netherlands)*, **59**, 1, (2008).
23. A. M. Florea and D. Büsselberg, *Cancers*, **3**, 1351, (2011).

24. S. Seng, Z. Liu, S. K. Chiu, T. Proverbs-Singh, G. Sonpavde, T. K. Choueiri, C. K. Tsao, M. Yu, N. M. Hahn, W. K. Oh and M. D. Galsky, *Journal of clinical oncology : official journal of the American Society of Clinical Oncology*, **30**, 4416, (2012).
25. W. Koizumi, H. Narahara, T. Hara, A. Takagane, T. Akiya, M. Takagi, K. Miyashita, T. Nishizaki, O. Kobayashi, W. Takiyama, Y. Toh, T. Nagaie, S. Takagi, Y. Yamamura, K. Yanaoka, H. Orita and M. Takeuchi, *The Lancet. Oncology*, **9**, 215, (2008).
26. S. Guo, Y. Wang, L. Miao, Z. Xu, C. M. Lin, Y. Zhang and L. Huang, *ACS Nano*, **7**, 9896, (2013).
27. C. A. Rabik and M. E. Dolan, *Cancer treatment reviews*, **33**, 9, (2007).
28. K. Cho, X. Wang, S. Nie, Z. G. Chen and D. M. Shin, *Clinical cancer research : an official journal of the American Association for Cancer Research*, **14**, 1310, (2008).
29. S. D. Brown, P. Nativo, J. A. Smith, D. Stirling, P. R. Edwards, B. Venugopal, D. J. Flint, J. A. Plumb, D. Graham and N. J. Wheate, *Journal of the American Chemical Society*, **132**, 4678, (2010).
30. D. Pissuwan, T. Niidome and M. B. Cortie, *Journal of controlled release : official journal of the Controlled Release Society*, **149**, 65, (2011).
31. L. Vigderman and E. R. Zubarev, *Advanced drug delivery reviews*, **65**, 663, (2013).
32. H. Besrour, B. Tangour, R. Linguerri and M. Hochlaf, *Spectrochimica acta. Part A, Molecular and biomolecular spectroscopy*, **217**, 278, (2019).
33. G. Ciofani, V. Raffa, A. Menciassi and P. Dario, *Journal of nanoscience and nanotechnology*, **8**, 6223, (2008).
34. G. Ciofani, *Expert opinion on drug delivery*, **7**, 889, (2010).
35. Y. Belmiloud, W. Djitli, H. Abdeldjebar, M. Abdelatif, B. Tangour and B. Meziane, *Superlattices and Microstructures*, (2016).
36. E. Duverger, T. Gharbi, E. Delabrousse and F. Picaud, *Physical Chemistry Chemical Physics*, **16**, 18425, (2014).
37. S. Roosta, S. J. Nikkhah, M. Sabzali and S. M. Hashemianzadeh, *RSC Advances*, **6**, 9344, (2016).
38. M. El Khalifi, E. Duverger, T. Gharbi, H. Boulahdour and F. Picaud, *Physical Chemistry Chemical Physics*, **17**, 30057, (2015).
39. M. El Khalifi, E. Duverger, T. Gharbi, H. Boulahdour and F. Picaud, *Analytical Methods*, **8**, 1367, (2016).
40. M. El Khalifi, J. Bentin, E. Duverger, T. Gharbi, H. Boulahdour and F. Picaud, *Physical Chemistry Chemical Physics*, **18**, 24994, (2016).
41. A. Mejri, D. Vardanega, B. Tangour, T. Gharbi and F. Picaud, *The Journal of Physical Chemistry B*, **119**, 604, (2015).
42. T. A. Hilder and J. M. Hill, *Current Applied Physics*, **8**, 258, (2008).
43. R. Bessrour, Y. Belmiloud, Z. Hosni and B. Tangour, *AIP Conference Proceedings*, **1456**, pp. 229, (2012).
44. A. Bianco and M. Prato, *Advanced Materials*, **15**, 1765, (2003).
45. Z. Hosni, R. Bessrour and B. Tangour, *Journal of Computational and Theoretical Nanoscience*, **11**, 318, (2014).
46. A. Chu, J. Cook, R. J. R. Heesom, J. L. Hutchison, M. L. H. Green and J. Sloan, *Chemistry of Materials*, **8**, 2751, (1996).
47. S. C. Tsang, Y. K. Chen, P. J. F. Harris and M. L. H. Green, *Nature*, **372**, 159, (1994).
48. Z. Wang, M. D. Shirley, S. T. Meikle, R. L. D. Whitby and S. V. Mikhalovsky, *Carbon*, **47**, 73, (2009).
49. E. Heister, C. Lamprecht, V. Neves, C. Tîlmaciu, L. Datas, E. Flahaut, B. Soula, P. Hinterdorfer, H. M. Coley, S. R. Silva and J. McFadden, *ACS Nano*, **4**, 2615, (2010).

50. H. Lee, S. Mall, V. Nalladega, S. Sathish, A. Roy and K. Lafdi, *Polymers and Polymer Composites*, **14**, 549, (2006).
51. K. A. Worsley, I. Kalinina, E. Bekyarova and R. C. Haddon, *Journal of the American Chemical Society*, **131**, 18153, (2009).
52. P. Mark and L. Nilsson, *The Journal of Physical Chemistry A*, **105**, 9954, (2001).
53. A. D. Becke, *The Journal of Chemical Physics*, **98**, 1372, (1993).
54. C. Lee, W. Yang and R. G. Parr, *Physical Review B*, **37**, 785, (1988).
55. S. H. Vosko, L. Wilk and M. Nusair, *Canadian Journal of Physics*, **59**, 1200, (1980).
56. P. J. Stephens, F. J. Devlin, C. F. Chabalowski and M. J. Frisch, *The Journal of Physical Chemistry*, **98**, 11623, (1994).
57. W. J. Hehre, R. Ditchfield and J. A. Pople, *The Journal of Chemical Physics*, **56**, 2257, (1972).
58. C. E. Check, T. O. Faust, J. M. Bailey, B. J. Wright, T. M. Gilbert and L. S. Sunderlin, *The Journal of Physical Chemistry A*, **105**, 8111, (2001).
59. L. Kalé, R. Skeel, M. Bhandarkar, R. Brunner, A. Gursoy, N. Krawetz, J. Phillips, A. Shinozaki, K. Varadarajan and K. Schulten, *Journal of Computational Physics*, **151**, 283, (1999).
60. A. B. Farimani, Y. Wu and N. R. Aluru, *Physical Chemistry Chemical Physics*, **15**, 17993, (2013).
61. W. L. Jorgensen, J. Chandrasekhar, J. D. Madura, R. W. Impey and M. L. Klein, *The Journal of Chemical Physics*, **79**, 926, (1983).
62. F. Sajadi and C. N. Rowley, *PeerJ*, **6**, e5472, (2018).
63. L. Lindsay and D. A. Broido, *Physical Review B*, **82**, 209903, (2010).
64. C. E. Faller, K. A. Reilly, R. D. Hills, Jr. and O. Guvench, *J Phys Chem B*, **117**, 518, (2013).
65. D. Rodriguez-Gomez, E. Darve and A. Pohorille, *J Chem Phys*, **120**, 3563, (2004).
66. J. Hénin, G. Fiorin, C. Chipot and M. L. Klein, *Journal of Chemical Theory and Computation*, **6**, 35, (2010).
67. E. Darve, D. Rodríguez-Gómez and A. Pohorille, *J Chem Phys*, **128**, 144120, (2008).
68. H. Sun, Y. Li, D. Li and T. Hou, *Journal of Chemical Information and Modeling*, **53**, 2376, (2013).
69. I. Pires de Oliveira, C. H. Lescano and G. De Nucci, *Chemical Biology & Drug Design*, **93**, 419, (2019).
70. H. Wang, X. Ren and F. Meng, *Molecular Simulation*, **42**, 56, (2016).
71. Nawal K. Khadka, X. Cheng, Chian S. Ho, J. Katsaras and J. Pan, *Biophysical Journal*, **108**, 2492, (2015).
72. C. Tripisciano, S. Costa, R. J. Kalenczuk and E. Borowiak-Palen, *The European Physical Journal B*, **75**, 141, (2010).
73. A. Guven, I. A. Rusakova, M. T. Lewis and L. J. Wilson, *Biomaterials*, **33**, 1455, (2012).
74. L. A. De Souza, H. F. Dos Santos, L. T. Costa and W. B. De Almeida, *Journal of inorganic biochemistry*, **178**, 134, (2018).
75. A. A. Bhirde, A. A. Sousa, V. Patel, A. A. Azari, J. S. Gutkind, R. D. Leapman and J. F. Rusling, *Nanomedicine*, **4**, 763, (2009).
76. E. Mehrjouei, H. Akbarzadeh, A. N. Shamkhali, M. Abbaspour, S. Salemi and P. Abdi, *Molecular Pharmaceutics*, **14**, 2273, (2017).
77. P. Wolski, K. Nieszporek and T. Panczyk, *Physical Chemistry Chemical Physics*, **19**, 9300, (2017).
78. P. Wolski, K. Nieszporek and T. Panczyk, *Langmuir*, **34**, 2543, (2018).
79. J. S. Camp and D. S. Sholl, *The Journal of Physical Chemistry C*, **120**, 1110, (2016).

Supplementary materials :

S1

- **Force Field parameters for CDDP molecule :**

Bonds	**Kb (kcal/mol/A^2)**	**Angles**	**Kb (kcal/mol/A^2)**
Pt-Cl (r_0= 2.3953Å)	101.059	Cl-Pt-Cl (θ_0= 93.38°)	39.642
Pt-N (r_0= 2.0809 Å)	138.132	N-Pt-N (θ_0= 90.72°)	41.184
N-H (r_0= 1.0261 Å)	435.375	Cl-Pt-N (θ_0= 87.95°)	45.144
		H-N-H (θ_0= 107.61°)	14.546
		H-N-Pt (θ_0= 109.93°)	19.507

- **Lennard-Jones parameters and partial charges :**

atom	**σ(Å) (Rmin/2)**	**ε(kcal/mol)**	**Partial charge**
Pt	1.3770	-0.0800	+0.104
Cl	1.9735	-0.2270	-0.403
N	1.9000	-0.0750	-0.896
H	1.4430	-0.0440	+0.418

S2

- **Force Field parameters for CNT :**

Bonds	**Kb (kcal/mol/A^2)**	**Angles**	**Kb (kcal/mol/A^2)**
C-C (r_0= 1.415Å)	600	C-C-C (θ_0= 120°)	350
C-O (r_0= 1.395 Å)	300	C-C-O (θ_0= 120°)	45
C-H (r_0= 1.415 Å)	600	H-O-C (θ_0= 119.47°)	35
H-O (r_0= 0.948 Å)	605	H-C-C (θ_0= 118.85°)	600

- **Lennard Jones parameters :**

atom	**σ(Å) (Rmin/2)**	**ε(kcal/mol)**
C	1.9474	-0.0660
H	1.459	-0.0150
O	1.721	-0.0750